The Second Lie-Group $SO_o(n,1)$ Used to Solve Ordinary Differential Equations

Chein-Shan Liu[1] & Wun-Sin Jhao[2]

[1] Department of Civil Engineering, National Taiwan University, Taipei, Taiwan

[2] Department of Systems Engineering & Naval Architecture, National Taiwan Ocean University, Keelung, Taiwan

Correspondence: Chein-Shan Liu, Department of Civil Engineering, National Taiwan University, Taipei, Taiwan. E-mail: liucs@ntu.edu.tw

Abstract

Liu (2001) derived the first augmented Lie-group $SO_o(n,1)$ symmetry for the nonlinear ordinary differential equations (ODEs): $\dot{\mathbf{x}} = \mathbf{f}(\mathbf{x}, t)$, and developed the corresponding group-preserving scheme (GPS). However, the earlier formulation did not consider the rotational effect of nonlinear ODEs. In this paper, we derive the second augmented Lie-group $SO_o(n,1)$ symmetry by taking the rotational effect into account. The numerical algorithm exhibits two solutions of the Lie-group $\mathbf{G} \in SO_o(n,1)$, depending on the sign of $\|\mathbf{f}\|^2\|\mathbf{x}\|^2 - 2(\mathbf{f} \cdot \mathbf{x})^2$, which means that the algorithm may be switched between two states, depending on $\mathbf{x}$. We give numerical examples to assess the new algorithm GPS2, which upon comparing with the GPS can raise the accuracy about three orders. It is interesting that for the chaotic system the signum function $\mathrm{sign}(\|\mathbf{f}\|^2\|\mathbf{x}\|^2 - 2(\mathbf{f} \cdot \mathbf{x})^2)$ is frequently switched between $+1$ and -1 in time.

Keywords: ordinary differential equations, chaotic system, Jordan dynamics, Lie-group $SO_o(n,1)$ symmetry, group-preserving scheme, Minkowski space

1. Introduction

There are a lot of numerical methods developed to solve the ordinary differential equations (ODEs), which are effective for most situations. However, when the ODEs possess special structures, like the conserved integrals and the Lie-group symmetries, those numerical methods designed for the general purpose cannot maintain the special structures, unless we can design a particular algorithm to do that. There was a substantial development in the Lie-group geometric integrators for solving ODEs (Iserles, Munthe-Kaas, Nørsett, & Zanna, 2000; Hairer, Lubich, & Wanner, 2002).

The majority of the Lie-group integrator is for providing a good performance algorithm that can enforce the orbit of numerical solution on the Lie-group manifold, which is a key way to retain qualitatively correct behavior, and also to reduce numerical errors. At the present time, there are many famous geometric integration methods, like the Crouch-Grossman, the RKMK, the Magnus, and the Fer methods. The existent studies clearly indicated that the Lie-group methods can improve the qualitative behavior and for a long term integration.

Basically, we have two approaches in the higher-order Lie-group integration methods. One is using the Lie group property and another is employing the Lie algebra structure, of which the geometric integrators developed by Hairer, Lubich and Wanner (2002), Iserles (1984), Iserles and Nørsett (1999), Iserles, Munthe-Kaas, Nørsett and Zanna (2000), Lee and Liu (2009), Munthe-Kaas (1998, 1999), and Zhang and Deng (2004, 2006) can be referred.

The remaining parts of this paper are organized and arranged as follows. In Section 2 we review the first augmented Lie-group $SO_o(n,1)$ symmetry derived by Liu (2001), and introduce the group-preserving scheme (GPS). Section 3 explores the concepts from the Jordan algebra and the Jordan dynamics to help us for finding the Lie-group $DSO(n)$ symmetry of nonlinear ODEs. The new developments of the second augmented Lie-group $SO_o(n,1)$ symmetry are described in Section 4, while the explicit formulas for the Lie-group $SO_o(n,1)$ integration method are derived in Section 5. In Section 6 we derive a novel explicit group-preserving scheme GPS2, which is used to solve nonlinear ODEs. In particular, we will emphasize the chaotic behavior of some well known chaotic systems

as being observed from the new method. Finally, the conclusions are drawn in Section 7.

2. The First Augmented Lie-Group Symmetry

Let us consider

$$\dot{\mathbf{x}} = \mathbf{f}(\mathbf{x}, t), \quad \mathbf{x}(0) = \mathbf{x}_0, \quad t \in \mathbb{R}, \quad \mathbf{x} \in \mathbb{R}^n, \tag{1}$$

which is an n-dimensional ODEs system for depicting an initial value problem. Generally speaking, the flow mapping given by

$$\boldsymbol{\phi}_t(\mathbf{x}_0) = \mathbf{x}(t; \mathbf{x}_0) \tag{2}$$

satisfies $\boldsymbol{\phi}_{t_1} \circ \boldsymbol{\phi}_{t_2} = \boldsymbol{\phi}_{t_1+t_2}$ as being a one-parameter semi-group. Although the ODEs possess such a property of being a semi-group, but in general, the ODEs do not necessarily have the Lie-group structure.

For Equation (1) we can consider an orientation of state vector (Liu, 2001):

$$\mathbf{n} := \frac{\mathbf{x}}{\|\mathbf{x}\|}, \tag{3}$$

where $\|\mathbf{x}\| := \sqrt{\mathbf{x} \cdot \mathbf{x}}$ is the length of $\mathbf{x}$, and the dot in $\mathbf{x} \cdot \mathbf{x}$ signifies the inner product. We suppose that $\mathbf{x} \neq \mathbf{0}$.

Upon using Equations (1) and (3), $\|\mathbf{x}\|$ is depicted by

$$\frac{d}{dt}\|\mathbf{x}\| = \frac{\dot{\mathbf{x}} \cdot \mathbf{x}}{\sqrt{\mathbf{x} \cdot \mathbf{x}}} = \mathbf{f}(\mathbf{x}, t) \cdot \mathbf{n}. \tag{4}$$

Then, from Equations (1), (3) and (4) it follows that

$$\dot{\mathbf{n}} = \frac{\mathbf{f}(\mathbf{x}, t)}{\|\mathbf{x}\|} - \left(\frac{\mathbf{f}(\mathbf{x}, t)}{\|\mathbf{x}\|} \cdot \mathbf{n} \right) \mathbf{n}. \tag{5}$$

Therefore, we have decomposed Equation (1) for $\mathbf{x}$ into Equations (4) and (5), respectively, for $\|\mathbf{x}\|$ and $\mathbf{n}$ with $\|\mathbf{x}\|\mathbf{n} = \mathbf{x}$.

From Equations (4) and (5) it follows that

$$\frac{d}{dt}(\|\mathbf{x}\|\mathbf{n}) = \mathbf{f}(\mathbf{x}, t), \tag{6}$$

which shows that the length $\|\mathbf{x}\|$ is an *integrating factor* of the governing Equation (5) for $\mathbf{n}$. Then, inserting $\|\mathbf{x}\|\mathbf{n} = \mathbf{x}$ into the above equation and combining with Equation (4) we can write a Lie-form system:

$$\dot{\mathbf{X}} = \mathbf{A}\mathbf{X}, \tag{7}$$

where

$$\mathbf{X} = \begin{bmatrix} \mathbf{x} \\ \|\mathbf{x}\| \end{bmatrix}, \quad \mathbf{A} := \begin{bmatrix} \mathbf{0}_{n \times n} & \frac{\mathbf{f}(\mathbf{x},t)}{\|\mathbf{x}\|} \\ \frac{\mathbf{f}^{\mathrm{T}}(\mathbf{x},t)}{\|\mathbf{x}\|} & 0 \end{bmatrix}. \tag{8}$$

$\mathbf{X}$ has one dimension higher than $\mathbf{x}$, and is called the augmented state vector, satisfying

$$\mathbf{X}^{\mathrm{T}}\mathbf{g}\mathbf{X} = 0, \tag{9}$$

where

$$\mathbf{g} = \begin{bmatrix} \mathbf{I}_n & \mathbf{0}_{n \times 1} \\ \mathbf{0}_{1 \times n} & -1 \end{bmatrix} \tag{10}$$

is the metric of the Minkowski space $\mathbb{M}^{n+1}$. $\mathbf{I}_n$ is an $n \times n$ identity matrix.

By employing the ODEs in Equation (7) with $\mathbf{A} \in so(n, 1)$, i.e.,

$$\mathbf{A}^{\mathrm{T}}\mathbf{g} + \mathbf{g}\mathbf{A} = \mathbf{0}, \tag{11}$$

Liu (2001, 2006) has developed a group-preserving scheme (GPS):

$$\mathbf{x}_{k+1} = \mathbf{x}_k + \eta_k \mathbf{f}_k, \tag{12}$$

$$\|\mathbf{x}_{k+1}\| = a_k \|\mathbf{x}_k\| + \frac{b_k}{\|\mathbf{f}_k\|} \mathbf{x}_k \cdot \mathbf{f}_k, \tag{13}$$

where

$$a_k := \cosh\left(\frac{h\|\mathbf{f}_k\|}{\|\mathbf{x}_k\|}\right), \quad b_k := \sinh\left(\frac{h\|\mathbf{f}_k\|}{\|\mathbf{x}_k\|}\right), \tag{14}$$

$$\eta_k := \frac{(a_k - 1)\mathbf{f}_k \cdot \mathbf{x}_k + b_k\|\mathbf{x}_k\|\|\mathbf{f}_k\|}{\|\mathbf{f}_k\|^2}, \tag{15}$$

and $h = \Delta t$ is a time increment. The values of $\mathbf{x}$ and $\mathbf{f}$ at a discrete time $t = t_k$ are simply denoted by $\mathbf{x}_k$ and $\mathbf{f}_k = \mathbf{f}(\mathbf{x}_k, t_k)$, respectively.

Because the above Lie-group $SO_o(n, 1)$ symmetry of Equation (7) is realized in the Minkowski space for the augmented state vectors, this kind symmetry may be termed the *augmented Lie-group symmetry*, and the Lie-group symmetry found by Liu (2001) is the *first augmented Lie-group symmetry* for Equation (1).

It is known that a matrix $\mathbf{A}$ of the real Lie algebra $so(n, 1)$ of the Lorentz group $SO_o(n, 1)$ has the general form (Hong & Liu, 1999):

$$\mathbf{A} = \begin{bmatrix} \mathbf{A}_s^s & \mathbf{A}_0^s \\ \mathbf{A}_s^0 & 0 \end{bmatrix}, \tag{16}$$

where

$$(\mathbf{A}_s^s)^{\mathrm{T}} = -\mathbf{A}_s^s, \quad \mathbf{A}_s^0 = (\mathbf{A}_0^s)^{\mathrm{T}}. \tag{17}$$

The matrix $\mathbf{A}$ in Equation (7) is a special case of Equation (16) with $\mathbf{A}_s^s = \mathbf{0}$ and $\mathbf{A}_0^s = \mathbf{f}/\|\mathbf{x}\|$. In this paper, we attempt to derive the *second augmented Lie-group symmetry* for Equation (1), of which the Lie-algebra is in the form of Equation (16) with $\mathbf{A}_s^s \neq \mathbf{0}$. This new method can generate a new algorithm which is better than the GPS. The following ODEs system:

$$\dot{\mathbf{X}} = \mathbf{A}(\mathbf{X}, t)\mathbf{X} \tag{18}$$

is termed a Lie-form system if $\mathbf{A}$ satisfies the properties of Lie-algebra.

3. The Jordan Structure

From the Jordan structure (Iordanescu, 2007, 2009) we can give a new aspect of Equation (5), and then the *second augmented Lie-group symmetry* for Equation (1) can be deduced. To derive the novel Lie-symmetry, we will use the Jordan algebra and the triple system developed by Liu (2000), who was the first one to develop a dynamical system based on the triple-vector $(\mathbf{y}, \mathbf{z}, \mathbf{u})$:

$$\dot{\mathbf{x}} = [\mathbf{y}, \mathbf{z}, \mathbf{u}] = \mathbf{y} \cdot \mathbf{z}\mathbf{u} - \mathbf{u} \cdot \mathbf{z}\mathbf{y}. \tag{19}$$

The triplet $\mathbf{y}$, $\mathbf{z}$ and $\mathbf{u}$ can be functions of $\mathbf{x}$ and t. Liu (2000) has shown that $\mathbf{y} \cdot \mathbf{z}\mathbf{u}$ is a conservative term, while $\mathbf{u} \cdot \mathbf{z}\mathbf{y}$ represents a dissipative term.

By using the Jordan dynamics in Equation (19) and using $\mathbf{n} \cdot \mathbf{n} = \|\mathbf{n}\|^2 = 1$, we can write Equation (5) to be

$$\dot{\mathbf{n}} = \left[\mathbf{n}, \mathbf{n}, \frac{\mathbf{f}}{\|\mathbf{x}\|}\right]. \tag{20}$$

Moreover, Equation (20) can be recast to

$$\dot{\mathbf{n}} = \left[\frac{\mathbf{f}}{\|\mathbf{x}\|} \otimes \mathbf{n} - \mathbf{n} \otimes \frac{\mathbf{f}}{\|\mathbf{x}\|}\right]\mathbf{n}, \tag{21}$$

where $\mathbf{u} \otimes \mathbf{y}$ is defined by $(\mathbf{u} \otimes \mathbf{y})\mathbf{z} = \mathbf{y} \cdot \mathbf{z}\mathbf{u}$, which is a dyad of $\mathbf{u}$ and $\mathbf{y}$. Due to

$$\left[\frac{\mathbf{f}}{\|\mathbf{x}\|} \otimes \mathbf{n} - \mathbf{n} \otimes \frac{\mathbf{f}}{\|\mathbf{x}\|}\right]^{\mathrm{T}} = -\left[\frac{\mathbf{f}}{\|\mathbf{x}\|} \otimes \mathbf{n} - \mathbf{n} \otimes \frac{\mathbf{f}}{\|\mathbf{x}\|}\right],$$

the Lie-group symmetry for Equation (21) is $SO(n)$.

The pair

$$\left(\frac{\mathbf{f}}{\|\mathbf{x}\|}, \mathbf{n}\right) \tag{22}$$

in Equation (21) is called a Jordan pair, and the following operation:

$$\frac{\mathbf{f}}{\|\mathbf{x}\|} \otimes \mathbf{n} - \mathbf{n} \otimes \frac{\mathbf{f}}{\|\mathbf{x}\|} \tag{23}$$

is called the Jordan cross product of the Jordan pair, which is an extension of the usual cross product of vectors in three-dimensional space $\mathbb{R}^3$.

From Equations (4) and (21) and $\mathbf{x} = \|\mathbf{x}\|\mathbf{n}$ we have

$$\dot{\mathbf{x}} = \frac{\mathbf{f} \cdot \mathbf{x}}{\|\mathbf{x}\|^2}\mathbf{x} + \left[\frac{\mathbf{f}}{\|\mathbf{x}\|} \otimes \frac{\mathbf{x}}{\|\mathbf{x}\|} - \frac{\mathbf{x}}{\|\mathbf{x}\|} \otimes \frac{\mathbf{f}}{\|\mathbf{x}\|}\right]\mathbf{x}, \tag{24}$$

which can be re-formulated as

$$\dot{\mathbf{x}} = [\mathbf{S} + \mathbf{W}]\mathbf{x}, \tag{25}$$

where

$$\mathbf{S} = \frac{\mathbf{f} \cdot \mathbf{x}}{\|\mathbf{x}\|^2}\mathbf{I}_n, \quad \mathbf{W} = \frac{\mathbf{f}}{\|\mathbf{x}\|} \otimes \frac{\mathbf{x}}{\|\mathbf{x}\|} - \frac{\mathbf{x}}{\|\mathbf{x}\|} \otimes \frac{\mathbf{f}}{\|\mathbf{x}\|}. \tag{26}$$

As shown by Liu (2013a), Equation (25) is equipped with a Lie-group $DSO(n)$ symmetry, with $\mathbf{Sx}$ rendering a dilation/contraction and $\mathbf{Wx}$ causing a rotation. It is interesting that the coefficient matrices $\mathbf{S}$ and $\mathbf{W}$ are fully determined by the Jordan pair in Equation (22); they are, respectively, the *inner product* and the *Jordan cross product* of the *Jordan pair*. Recently, Liu (2013a) has developed a $DSO(n)$ Lie-group algorithm based on Equation (25).

4. The Second Augmented Lie-Group Symmetry

By the definition of Equation (3), Equation (4) can be written as

$$\frac{d}{dt}\|\mathbf{x}\| = \mathbf{f} \cdot \frac{\mathbf{x}}{\|\mathbf{x}\|}, \tag{27}$$

and then Equations (24) and (27) can be written together as

$$\frac{d}{dt}\begin{bmatrix} \mathbf{x} \\ \|\mathbf{x}\| \end{bmatrix} = \begin{bmatrix} \mathbf{W} & \frac{(\mathbf{f}\cdot\mathbf{x})\mathbf{x}}{\|\mathbf{x}\|^3} \\ \frac{(\mathbf{f}\cdot\mathbf{x})\mathbf{x}^{\mathrm{T}}}{\|\mathbf{x}\|^3} & 0 \end{bmatrix}\begin{bmatrix} \mathbf{x} \\ \|\mathbf{x}\| \end{bmatrix}. \tag{28}$$

Moreover, in terms of

$$\mathbf{X} := \begin{bmatrix} \mathbf{x} \\ \|\mathbf{x}\| \end{bmatrix}, \quad \mathbf{B} := \begin{bmatrix} \mathbf{W} & \frac{(\mathbf{f}\cdot\mathbf{x})\mathbf{x}}{\|\mathbf{x}\|^3} \\ \frac{(\mathbf{f}\cdot\mathbf{x})\mathbf{x}^{\mathrm{T}}}{\|\mathbf{x}\|^3} & 0 \end{bmatrix}, \tag{29}$$

we can find three inherent structures about Equation (28):

$$\text{Cone: } \mathbf{X}^{\mathrm{T}}\mathbf{g}\mathbf{X} = 0, \tag{30}$$

$$\text{Lie-algebra: } \mathbf{B} \in so(n, 1), \quad \mathbf{B}^{\mathrm{T}}\mathbf{g} + \mathbf{g}\mathbf{B} = \mathbf{0}, \tag{31}$$

$$\text{Lie-group: } \mathbf{G} \in SO_o(n, 1), \quad \mathbf{G}^{\mathrm{T}}\mathbf{g}\mathbf{G} = \mathbf{g}, \tag{32}$$

where $\mathbf{g} := \text{diag}(\mathbf{I}_n, -1)$ is a signature $(n, 1)$ metric tensor, and $\mathbf{G}$ is the Lie-group generated from $\mathbf{B}$, which can be expressed as

$$\mathbf{G} = \begin{bmatrix} \mathbf{G}_s^s & \mathbf{G}_0^s \\ \mathbf{G}_s^0 & G_0^0 \end{bmatrix}. \tag{33}$$

In the above, $\mathbf{G}_s^s$ is an $n \times n$ matrix, $\mathbf{G}_0^s$ is an $n \times 1$ matrix, $\mathbf{G}_s^0$ is an $1 \times n$ matrix, and G_0^0 is a scalar. Corresponding to the first augmented Lie-group symmetry found by Liu (2001), the above Lie-group symmetry is the *second augmented Lie-group symmetry* in the Minkowski space $\mathbb{M}^{n+1}$ for Equation (1).

By using Equation (33) we can identify two types internal symmetries for $\mathbf{n}$ and $\mathbf{x}$, respectively:

$$\mathbf{n}(t) = \frac{\mathbf{G}_s^s\|\mathbf{x}_0\|\mathbf{n}_0 + \mathbf{G}_0^s\|\mathbf{x}_0\|}{\mathbf{G}_s^0\|\mathbf{x}_0\|\mathbf{n}_0 + G_0^0\|\mathbf{x}_0\|}, \tag{34}$$

$$\mathbf{x}(t) = \mathbf{G}_s^s\mathbf{x}_0 + \mathbf{G}_0^s\|\mathbf{x}_0\|, \tag{35}$$

where $\mathbf{x}_0$ and $\mathbf{n}_0$ denote, respectively, the initial values of $\mathbf{x}$ and $\mathbf{n}$. It can be seen that the symmetry for $\mathbf{n}$ is more complex than that for $\mathbf{x}$, because its symmetry is a projective type. On the other hand, the above two Lie-group transformations are different from the $SO(n)$ for $\mathbf{n}$ as shown in Equation (21), and the $DSO(n)$ for $\mathbf{x}$ as explored by Liu (2013a). While the Lie-group symmetry for $\mathbf{n}$ in Equation (34) is a projective type of $SO_o(n, 1)$, denoted by $PSO_o(n, 1)$, the Lie-group symmetry for $\mathbf{x}$ in Equation (35) is a Poincaré type: a Minkowskian rotation $\mathbf{G}_s^s\mathbf{x}_0$ follows by an Euclidean translation $\|\mathbf{x}_0\|\mathbf{G}_0^s$.

It can be seen that the augmented coefficient matrix $\mathbf{B}$ of Equation (28) is fully determined by the Jordan pair (22) with

$$\mathbf{B} = \left[\begin{array}{cc} \mathbf{W} & \mathbf{Sn} \\ (\mathbf{Sn})^{\mathrm{T}} & 0 \end{array} \right] = \left[\begin{array}{cc} \frac{\mathbf{f}}{\|\mathbf{x}\|} \otimes \mathbf{n} - \mathbf{n} \otimes \frac{\mathbf{f}}{\|\mathbf{x}\|} & \left(\frac{\mathbf{f}}{\|\mathbf{x}\|} \cdot \mathbf{n} \right) \mathbf{n} \\ \left(\frac{\mathbf{f}}{\|\mathbf{x}\|} \cdot \mathbf{n} \right) \mathbf{n}^{\mathrm{T}} & 0 \end{array} \right], \tag{36}$$

where the scalar in the symmetric part is the inner product of the Jordan pair, and the skew-symmetric part is the Jordan cross product of the Jordan pair.

Now we can observe that the above $\mathbf{B}$ is of the general form in Equation (16), as being a full Lie-algebra of $so(n, 1)$. Upon comparing the above $\mathbf{B}$ with the coefficient matrix $\mathbf{A}$ in Equation (7):

$$\mathbf{A} = \left[\begin{array}{cc} \mathbf{0}_{n \times n} & \frac{\mathbf{f}}{\|\mathbf{x}\|} \\ \frac{\mathbf{f}^{\mathrm{T}}}{\|\mathbf{x}\|} & 0 \end{array} \right], \tag{37}$$

the matrix $\mathbf{B}$ includes a skew-symmetric part $\mathbf{W}$, which is absent in $\mathbf{A}$. It can take the rotational effect of nonlinear dynamical flow into account.

From Equation (24), by using the dyadic operation for the last term, we have

$$\dot{\mathbf{x}} = \frac{\mathbf{f} \cdot \mathbf{x}}{\|\mathbf{x}\|^2} \mathbf{x} + \left[\frac{\mathbf{f}}{\|\mathbf{x}\|} \otimes \frac{\mathbf{x}}{\|\mathbf{x}\|} \right] \mathbf{x} - \frac{\mathbf{x}}{\|\mathbf{x}\|} \frac{\mathbf{f} \cdot \mathbf{x}}{\|\mathbf{x}\|}. \tag{38}$$

Then the first term and the last term are cancelled out, which leads to

$$\dot{\mathbf{x}} = \left[\frac{\mathbf{f}}{\|\mathbf{x}\|} \otimes \frac{\mathbf{x}}{\|\mathbf{x}\|} \right] \mathbf{x}. \tag{39}$$

This ODEs system is the most simple Lie-form representation of Equation (1). Liu (2013b) has developed a $GL(n, \mathbb{R})$ Lie-group symmetry and used it to develop a Lie-group algorithm based on Equation (39). Up to here we have derived four types Lie-group symmetries about Equation (1).

5. Two Solutions of G

From Equation (28) we can develop a numerical scheme, by supposing that the Jordan pair

$$(\mathbf{a}, \mathbf{b}) = \left(\frac{\bar{\mathbf{f}}}{\|\bar{\mathbf{x}}\|}, \bar{\mathbf{n}} \right) \tag{40}$$

is constant within a small time step h, where the bar means that they are taking values at a mid-point $\bar{t} \in [0, h]$.

From Equation (4), Liu (2013a) has written the ODE for the length to be

$$\frac{d}{dt}\|\mathbf{x}\| = \left(\frac{\mathbf{f}}{\|\mathbf{x}\|} \cdot \mathbf{n} \right) \|\mathbf{x}\|. \tag{41}$$

Under the above assumption in Equation (40) we can obtain

$$\|\mathbf{x}(t)\| = \exp(\mathbf{a} \cdot \mathbf{b}t)\|\mathbf{x}_0\|. \tag{42}$$

However, a more subtle representation of the ODE for the length is in terms of the Jordan pair (40):

$$\frac{d}{dt}\|\mathbf{x}\| = \mathbf{a} \cdot \mathbf{bb} \cdot \mathbf{x}, \tag{43}$$

which is the second equation in Equation (28). Below, we will derive a new symmetry based on Equation (28).

From Equations (28) and (40) it follows that

$$\dot{\mathbf{x}} = \mathbf{b} \cdot \mathbf{x}\mathbf{a} - \mathbf{a} \cdot \mathbf{x}\mathbf{b} + \|\mathbf{x}\|\mathbf{a} \cdot \mathbf{b}\mathbf{b}. \tag{44}$$

Let

$$z = \mathbf{a} \cdot \mathbf{x}, \quad w = \mathbf{b} \cdot \mathbf{x}, \quad y = \|\mathbf{x}\|, \tag{45}$$
$$c_0 = \mathbf{a} \cdot \mathbf{b}, \tag{46}$$

and Equations (44) and (43) become

$$\dot{\mathbf{x}} = w\mathbf{a} - z\mathbf{b} + c_0 y\mathbf{b}, \tag{47}$$
$$\dot{y} = c_0 w. \tag{48}$$

Consequently, we can derive

$$\frac{d}{dt}\begin{pmatrix} z \\ w \\ y \end{pmatrix} = \begin{pmatrix} -c_0 & a_0^2 & c_0^2 \\ -1 & c_0 & c_0 \\ 0 & c_0 & 0 \end{pmatrix}\begin{pmatrix} z \\ w \\ y \end{pmatrix}, \tag{49}$$

where $a_0 = \|\mathbf{a}\|$.

For the special case with $c_0 = 0$ we have

$$\mathbf{x}(t) = \mathbf{x}_0 + \left[\frac{[\cos(\omega t) - 1]z_0}{\omega^2} + \frac{\sin(\omega t)w_0}{\omega} \right]\mathbf{a} + \left[[\cos(\omega t) - 1]w_0 - \frac{\sin(\omega t)z_0}{\omega} \right]\mathbf{b}, \tag{50}$$

where $\omega = \|\mathbf{a}\|$, $z_0 = \mathbf{a} \cdot \mathbf{x}_0$ and $w_0 = \mathbf{b} \cdot \mathbf{x}_0$. For this case $\|\mathbf{x}\|$ is a constant.

In Appendix A we give a detailed derivation of the solutions for (z, w, y) with $c_0 \neq 0$. Depending on the signum function of

$$\text{sign}(a_0^2 - 2c_0^2) = \frac{a_0^2 - 2c_0^2}{|a_0^2 - 2c_0^2|} = \text{sign}(\|\mathbf{f}\|^2\|\mathbf{x}\|^2 - 2(\mathbf{f} \cdot \mathbf{x})^2), \tag{51}$$

there exist two different types solutions of (z, w, y). We give the solutions of $\mathbf{X}(t) = (\mathbf{x}(t), \|\mathbf{x}(t)\|)^{\mathrm{T}}$ and $\mathbf{G}$ in the following.

5.1 The Solution of $\mathbf{X}(t)$ When sign $= -1$

For the case with $a_0^2 - 2c_0^2 < 0$, inserting Equation (A5) for z, w and y into Equation (47) and integrating it we have

$$\mathbf{x}(t) = \mathbf{x}_0 + [G_1(t)z_0 + G_2(t)w_0 + G_5(t)\|\mathbf{x}_0\|]\mathbf{a} + [G_3(t)z_0 + G_4(t)w_0 + G_6(t)\|\mathbf{x}_0\|]\mathbf{b}, \tag{52}$$

where

$$G_1(t) = \frac{c_2[1 - f_2(t)]}{c_0^2},$$
$$G_2(t) = \frac{c_2[f_2(t) - 1]}{c_0} + \frac{f_1(t)}{\omega},$$
$$G_3(t) = \frac{d_1[1 - f_2(t)]}{\omega} - \frac{(c_2 + c_3)f_1(t)}{\omega},$$
$$G_4(t) = \frac{(c_0^2 - d_2\omega)[f_2(t) - 1]}{\omega^2} + \frac{(c_0 c_2 - d_3)f_1(t)}{\omega},$$
$$G_5(t) = \frac{c_2[f_2(t) - 1]}{c_0},$$
$$G_6(t) = \frac{c_0 f_1(t)}{\omega} - c_2[f_2(t) - 1], \tag{53}$$

in which $\omega = \sqrt{2c_0^2 - a_0^2}$, $f_1(t) = \sinh(\omega t)$, and $f_2(t) = \cosh(\omega t)$.

On the other hand, by using the last equation in Equation (A5) and inserting $z_0 = \mathbf{a} \cdot \mathbf{x}_0$, and $w_0 = \mathbf{b} \cdot \mathbf{x}_0$ we can obtain

$$\|\mathbf{x}(t)\| = -G_5(t)\mathbf{a} \cdot \mathbf{x}_0 + G_7(t)\mathbf{b} \cdot \mathbf{x}_0 + [c_3 + c_2 f_2(t)]\|\mathbf{x}_0\|, \tag{54}$$

where

$$G_7(t) = \frac{c_0 f_1(t)}{\omega} + c_2[f_2(t) - 1].\qquad(55)$$

5.2 The Solution of $\mathbf{X}(t)$ When sign = +1

Next we consider the case with $a_0^2 - 2c_0^2 > 0$, of which by inserting Equation (A9) for z, w and y into Equation (47) and integrating it, render

$$\mathbf{x}(t) = \mathbf{x}_0 + [g_1(t)z_0 + g_2(t)w_0 + g_5(t)\|\mathbf{x}_0\|]\mathbf{a} + [g_3(t)z_0 + g_4(t)w_0 + g_6(t)\|\mathbf{x}_0\|]\mathbf{b},\qquad(56)$$

where

$$g_1(t) = \frac{c_2[1 - f_4(t)]}{c_0^2},$$

$$g_2(t) = \frac{c_2[f_4(t) - 1]}{c_0} + \frac{f_3(t)}{\omega},$$

$$g_3(t) = \frac{d_1[f_4(t) - 1]}{\omega} - \frac{(c_2 + c_3)f_3(t)}{\omega},$$

$$g_4(t) = \frac{(c_0^2 - d_2\omega)[1 - f_4(t)]}{\omega^2} + \frac{(c_0 c_2 - d_3)f_3(t)}{\omega},$$

$$g_5(t) = \frac{c_2[f_4(t) - 1]}{c_0},$$

$$g_6(t) = \frac{c_0 f_3(t)}{\omega} - c_2[f_4(t) - 1],\qquad(57)$$

in which $\omega = \sqrt{a_0^2 - 2c_0^2}$, $f_3(t) = \sin(\omega t)$, and $f_4(t) = \cos(\omega t)$.

By using the last equation in Equation (A9) and inserting $z_0 = \mathbf{a} \cdot \mathbf{x}_0$, and $w_0 = \mathbf{b} \cdot \mathbf{x}_0$ we can obtain

$$\|\mathbf{x}(t)\| = -g_5(t)\mathbf{a} \cdot \mathbf{x}_0 + g_7(t)\mathbf{b} \cdot \mathbf{x}_0 + [c_3 + c_2 f_4(t)]\|\mathbf{x}_0\|,\qquad(58)$$

where

$$g_7(t) = \frac{c_0 f_3(t)}{\omega} + c_2[f_4(t) - 1].\qquad(59)$$

To find $\mathbf{G}$ in Equation (33), which corresponding to a constant matrix $\mathbf{B}$ in Equation (36), is equivalent to find the augmented state transition matrix from $\mathbf{X}_0$ to $\mathbf{X}(t)$.

5.3 The Solution of $\mathbf{G}$ When sign = +1

From Equations (56) and (58) we can obtain

$$\mathbf{G}_s^s = \mathbf{I}_n + g_1(t)\mathbf{a}\mathbf{a}^{\mathrm{T}} + g_2(t)\mathbf{a}\mathbf{b}^{\mathrm{T}} + g_3(t)\mathbf{b}\mathbf{a}^{\mathrm{T}} + g_4(t)\mathbf{b}\mathbf{b}^{\mathrm{T}},$$
$$\mathbf{G}_0^s = g_5(t)\mathbf{a} + g_6(t)\mathbf{b},$$
$$\mathbf{G}_s^0 = -g_5(t)\mathbf{a}^{\mathrm{T}} + g_7(t)\mathbf{b}^{\mathrm{T}},$$
$$G_0^0 = c_3 + c_2 f_4(t).\qquad(60)$$

Besides the property in Equation (32), we can prove that

$$G_0^0 \geq 1,\qquad(61)$$

which is important in the numerical scheme to preserve the orientation of $\|\mathbf{x}\| > 0$. From Equation (A10) we have

$$c_3 + c_2 = 1.$$

By using

$$c_2 = \frac{c_0}{c_0 - c_1}, \quad c_3 = -\frac{c_1 c_2}{c_0},$$

we can obtain

$$1 - c_2 = 1 - \frac{c_0}{c_0 - c_1} = -\frac{c_1}{c_0}\frac{c_0}{c_0 - c_1} = -\frac{c_1 c_2}{c_0} = c_3,$$

which leads to $c_3 + c_2 = 1$.

Because of

$$\frac{1}{c_2} = -\frac{\omega^2}{c_0^2} < 0, \quad 0 < \cos(\omega t) \leq 1,$$

we have

$$G_0^0 = c_3 + c_2 f_4(t) = c_3 + c_2 \cos(\omega t) \geq c_3 + c_2 = 1.$$

This ends the proof of Equation (61).

5.4 The Solution of **G** *When sign* $= -1$

For the case with $a_0^2 - 2c_0^2 < 0$ we have a similar **G** with

$$\begin{aligned}
\mathbf{G}_s^s &= \mathbf{I}_n + G_1(t)\mathbf{aa}^{\mathrm{T}} + G_2(t)\mathbf{ab}^{\mathrm{T}} + G_3(t)\mathbf{ba}^{\mathrm{T}} + G_4(t)\mathbf{bb}^{\mathrm{T}}, \\
\mathbf{G}_0^s &= G_5(t)\mathbf{a} + G_6(t)\mathbf{b}, \\
\mathbf{G}_s^0 &= -G_5(t)\mathbf{a}^{\mathrm{T}} + G_7(t)\mathbf{b}^{\mathrm{T}}, \\
G_0^0 &= c_3 + c_2 f_2(t) \geq 1.
\end{aligned} \tag{62}$$

The last inequality follows from

$$c_3 + c_2 = 1, \quad \frac{1}{c_2} = \frac{\omega^2}{c_0^2} > 0, \quad f_2 = \cosh(\omega t) \geq 1,$$

by using Equation (A6).

Up to here we have derived two different **G**'s as shown in Equations (60) and (62). For the ODEs: $\dot{\mathbf{x}} = \mathbf{f}(\mathbf{x}, t)$, depending on the value of $\mathrm{sign}(\|\mathbf{f}\|^2\|\mathbf{x}\|^2 - 2(\mathbf{f} \cdot \mathbf{x})^2)$ we may alternatively use Equation (52) or Equation (56) to compute the solution of $\mathbf{x}(t)$ step-by-step. Hence, we have developed a *two-phase Lie-group algorithm* to solve Equation (1), where the algorithm may be switched between two states detected by the solution of **x**.

6. Numerical Examples

In order to distinct the present method from the group-preserving scheme (GPS) developed by Liu (2001), we may call the new algorithm to be the second GPS, simply denoted by GPS2, which is summarized as follows.

(i) Give an initial value of $\mathbf{x}_0$ at an initial time $t = t_0$ and a time stepsize h.

(ii) For $k = 0, 1, \ldots$, we repeat the following computations to a specified terminal time $t = t_f$:

$$\begin{aligned}
\mathbf{a}_k &= \frac{\mathbf{f}_k}{\|\mathbf{x}_k\|}, \\
\mathbf{b}_k &= \frac{\mathbf{x}_k}{\|\mathbf{x}_k\|}, \\
a_0^k &= \|\mathbf{a}_k\|, \\
c_0^k &= \mathbf{a}_k \cdot \mathbf{b}_k, \\
z_0^k &= \mathbf{a}_k \cdot \mathbf{x}_k, \\
w_0^k &= \mathbf{b}_k \cdot \mathbf{x}_k, \\
\mathrm{sign} &= \frac{(a_0^k)^2 - 2(c_0^k)^2}{|(a_0^k)^2 - 2(c_0^k)^2|},
\end{aligned}$$

$$\text{if } \text{sign} = +1, \begin{cases} \omega_k = \sqrt{(a_0^k)^2 - 2(c_0^k)^2}, \\ c_1^k = \frac{(c_0^k)^2 + \omega_k^2}{c_0^k}, \\ c_2^k = \frac{c_0^k}{c_0^k - c_1^k}, \\ c_3^k = -\frac{c_1^k c_2^k}{c_0^k}, \\ d_1^k = \frac{c_2^k \omega_k}{c_0^k}, \\ d_2^k = \frac{c_0^k c_1^k}{\omega_k} - c_2^k \omega_k, \\ d_3^k = c_0^k + c_1^k c_2^k, \\ a_k = \sin(\omega_k h), \\ b_k = \cos(\omega_k h), \\ g_3^k = \frac{d_1^k(b_k - 1)}{\omega_k} - \frac{(c_2^k + c_3^k)a_k}{\omega_k}, \\ g_4^k = \frac{[(c_0^k)^2 - d_2^k \omega_k](1 - b_k)}{\omega_k^2} + \frac{(c_0^k c_2^k - d_3^k)a_k}{\omega_k}, \end{cases} \tag{63}$$

$$\text{if } \text{sign} = -1, \begin{cases} \omega_k = \sqrt{2(c_0^k)^2 - (a_0^k)^2}, \\ c_1^k = \frac{(c_0^k)^2 - \omega_k^2}{c_0^k}, \\ c_2^k = \frac{c_0^k}{c_0^k - c_1^k}, \\ c_3^k = -\frac{c_1^k c_2^k}{c_0^k}, \\ d_1^k = -\frac{c_2^k \omega_k}{c_0^k}, \\ d_2^k = \frac{c_0^k c_1^k}{\omega_k} + c_2^k \omega_k, \\ d_3^k = c_0^k + c_1^k c_2^k, \\ a_k = \sinh(\omega_k h), \\ b_k = \cosh(\omega_k h), \\ g_3^k = \frac{d_1^k(1 - b_k)}{\omega_k} - \frac{(c_2^k + c_3^k)a_k}{\omega_k}, \\ g_4^k = \frac{[(c_0^k)^2 - d_2^k \omega_k](b_k - 1)}{\omega_k^2} + \frac{(c_0^k c_2^k - d_3^k)a_k}{\omega_k}, \end{cases} \tag{64}$$

$$g_1^k = \frac{c_2^k(1 - b_k)}{(c_0^k)^2},$$

$$g_2^k = \frac{c_2^k(b_k - 1)}{c_0^k} + \frac{a_k}{\omega_k},$$

$$g_5^k = \frac{c_2^k(b_k - 1)}{c_0^k},$$

$$g_6^k = \frac{c_0^k a_k}{\omega_k} - c_2^k(b_k - 1),$$

$$\mathbf{x}_{k+1} = \mathbf{x}_k + (g_1^k z_0^k + g_2^k w_0^k + g_5^k \|\mathbf{x}_k\|)\mathbf{a}_k + (g_3^k z_0^k + g_4^k w_0^k + g_6^k \|\mathbf{x}_k\|)\mathbf{b}_k. \tag{65}$$

We may see that the most nonlinear ODEs fall into the first class with sign = +1 and use Equation (63) for the numerical integration, because in Equation (63) there are $\sin(\omega_k h)$ and $\cos(\omega_k h)$, while that in Equation (64) there are $\sinh(\omega_k h)$ and $\cosh(\omega_k h)$. However, for the chaotic system the situation is quite different, with Equations (63) and (64) both being used in the numerical integration. We use the following examples to assess the performance of the GPS2.

6.1 Example 1

Let us consider the following periodic system:

$$\begin{aligned} \dot{x}_1 &= x_2, \quad x_1(0) = 0, \\ \dot{x}_2 &= -2.25x_1 - (x_1 - 1.5\sin t)^3 + 2\sin t, \quad x_2(0) = 1.59929. \end{aligned} \tag{66}$$
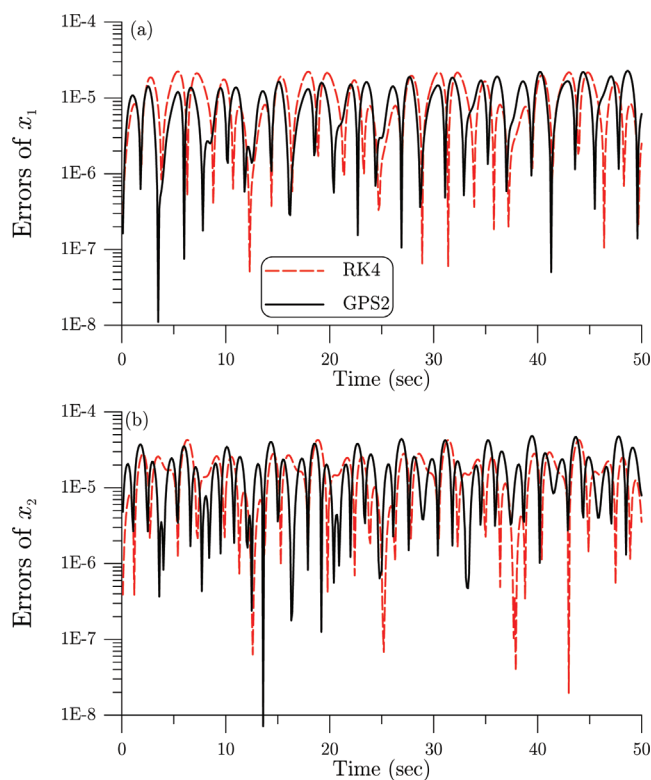
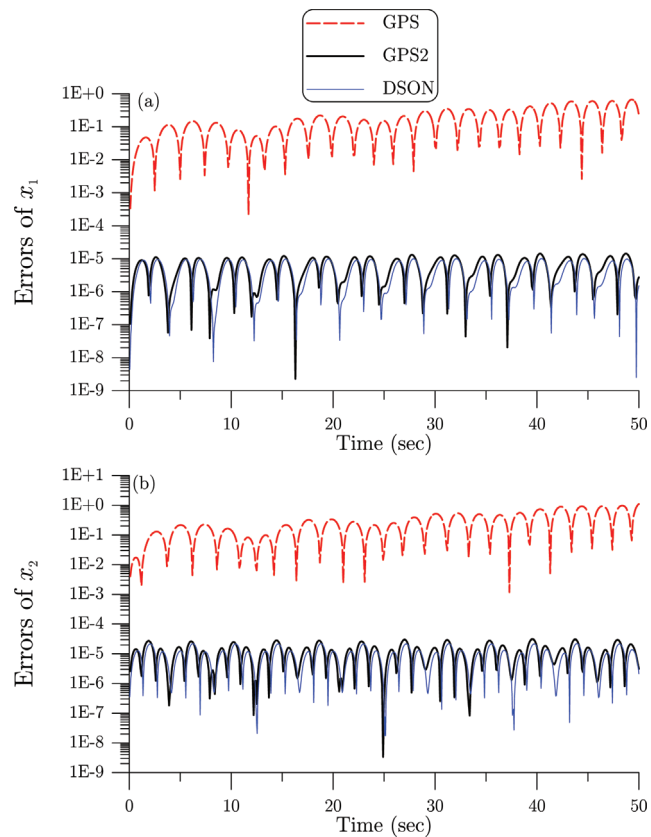Figure 1. For Example 1 with stepsize $h = 0.1$, the numerical errors of GPS2 and RK4

Figure 2. For Example 1 with stepsize $h = 0.01$, the numerical errors of GPS, DSON and GPS2

The exact solutions are

$$x_1(t) = 1.59941 \sin t - 0.00004 \sin 3t,$$
$$x_2(t) = 1.59941 \cos t - 0.00012 \cos 3t. \tag{67}$$

In Figure 1 we compare the numerical errors obtained by the GPS2 and the RK4, both using a stepsize $h = 0.1$. Under the stepsize $h = 0.1$, the GPS2 is better than RK4, while the GPS is failure. Under a small stepsize $h = 0.01$, these two schemes of GPS2 and RK4 have the same accuracy in the orders of $10^{-9} - 10^{-5}$. In Figure 2 we compare the numerical errors obtained by the GPS2, the $DS O(n)$ method (Liu, 2013a), and the GPS under the same stepsize $h = 0.01$, of which we can find that the $DS O(n)$ and the GPS2 method is much better than the GPS with the accuracy being raised three to four orders. For this system, the signum function defined by Equation (51) is $+1$, because the solutions are bounded.

6.2 Example 2

Then we consider

$$\ddot{x} = -\dot{x}^2 - x + \ln t, \quad x(1) = 0, \ \dot{x}(1) = 1, \tag{68}$$

which can be recast to

$$\dot{x}_1 = x_2, \quad x_1(1) = 0,$$
$$\dot{x}_2 = -x_1 - x_2^2 + \ln t, \quad x_2(1) = 1, \tag{69}$$

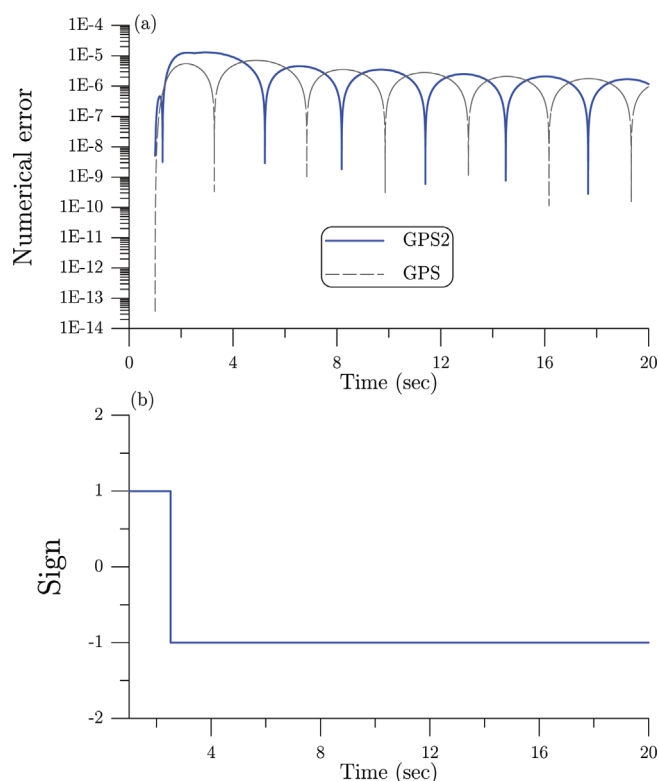and has the solution:

$$x(t) = \ln t. \tag{70}$$

Figure 3. For Example 2 with stepsize $h = 0.001$, (a) the numerical errors of GPS and GPS2, and (b) showing the sign function

We use $h = 0.001$. In Figure 3(a) the numerical errors obtained by GPS and GPS2 are compared. The accuracy of the above two methods are the same under a small time stepsize. In Figure 3(b) we show the signum function defined by Equation (51) for this system, which is regular and is changed from $+1$ to -1. For this system the solution $x(t) = \ln t$ is unbounded, such that after a certain time the signum function becomes -1.

This example motivates us to prove the following result. If Equation (1) satisfies

$$\mathbf{f}(\mathbf{x}(t_0), t_0) \cdot \mathbf{x}(t_0) > 0, \quad \text{and} \quad \text{sign}(\|\mathbf{f}\|^2 \|\mathbf{x}\|^2 - 2(\mathbf{f} \cdot \mathbf{x})^2) = -1, \ \forall t \geq t_0,$$
$$\text{then} \quad \mathbf{x}(t) \to \infty, \ t \to \infty. \tag{71}$$

There are two disconnected sets of $\|\mathbf{f}\|^2 \|\mathbf{x}\|^2 - 2(\mathbf{f} \cdot \mathbf{x})^2 < 0$:

$$\mathbf{f} \cdot \mathbf{x} < -\frac{1}{\sqrt{2}} \|\mathbf{f}\| \|\mathbf{x}\|, \quad \mathbf{f} \cdot \mathbf{x} > \frac{1}{\sqrt{2}} \|\mathbf{f}\| \|\mathbf{x}\|,$$

where the first case is impossible because it contradicts to $\mathbf{f}(\mathbf{x}(t_0), t_0) \cdot \mathbf{x}(t_0) > 0$. Then under the condition of $\text{sign}(\|\mathbf{f}\|^2 \|\mathbf{x}\|^2 - 2(\mathbf{f} \cdot \mathbf{x})^2) = -1$, it is always

$$\mathbf{f} \cdot \mathbf{x} > \frac{1}{\sqrt{2}} \|\mathbf{f}\| \|\mathbf{x}\|, \quad \forall t \geq t_0, \tag{72}$$

because the two sets are disconnected, and from the second set to the first set it must be $\text{sign}(\|\mathbf{f}\|^2 \|\mathbf{x}\|^2 - 2(\mathbf{f} \cdot \mathbf{x})^2) = +1$ on some time interval. Then, using Equations (27) and (72) we have

$$\frac{d}{dt} \|\mathbf{x}\| > \frac{1}{\sqrt{2}} \|\mathbf{f}\| > 0, \tag{73}$$

which means that the length grows with time. Thus, Equation (71) is proven.

6.3 Example 3

We consider an index 3 differential algebraic equations system, which describes the position of a particle on a circular track:

$$\ddot{u}_1 = 2u_2 + \lambda u_1, \tag{74}$$
$$\ddot{u}_2 = -2u_1 + \lambda u_2, \tag{75}$$
$$u_1^2 + u_2^2 = 1. \tag{76}$$

For $(u_1(0), u_2(0)) = (0, 1)$, $\lambda(0) = 0$, the exact solution is $u_1(t) = \sin t^2$, $u_2(t) = \cos t^2$ and $\lambda(t) = -4t^2$.

If we let $x_1 = u_1$, $x_2 = \dot{u}_1$, $x_3 = u_2$ and $x_4 = \dot{u}_2$, then through some derivations we find that the above system can be transformed to a system of ODEs:

$$\dot{x}_1 = x_2, \tag{77}$$
$$\dot{x}_2 = 2x_3 - x_1(x_2^2 + x_4^2), \tag{78}$$
$$\dot{x}_3 = x_4, \tag{79}$$
$$\dot{x}_4 = -2x_1 - x_3(x_2^2 + x_4^2), \tag{80}$$

which is subjecting to a constraint on (x_1, x_3):

$$x_1^2 + x_3^2 = 1, \tag{81}$$

and the Lagrange multiplier λ is calculated by

$$\lambda = -x_2^2 - x_4^2. \tag{82}$$

In Figure 4 we compare the numerical errors of u_1, u_2 and λ obtained by the GPS and GPS2 both with $h = 0.002$. It can be seen that the accuracy is in the order of h, and the GPS gradually tends to be unstable and blows up after $t = 6$ sec. For this system, the signum function defined by Equation (51) is +1.
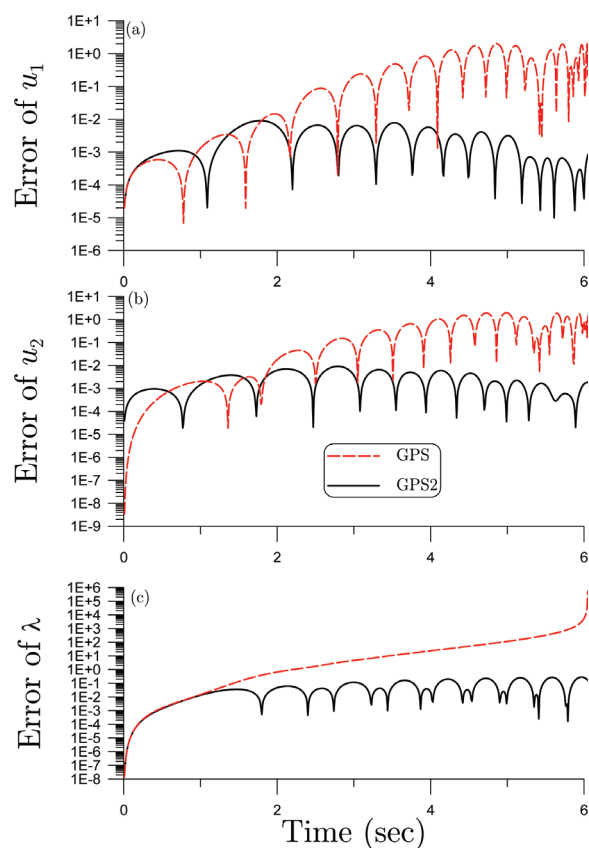
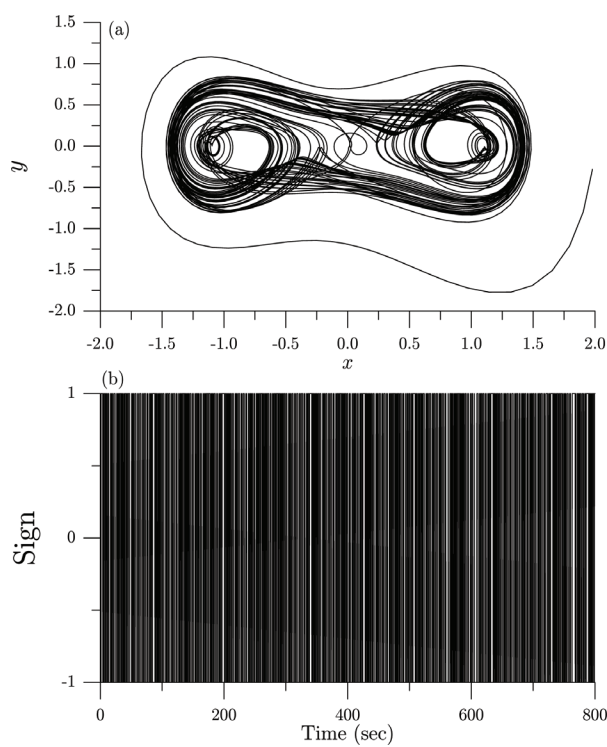Figure 4. For Example 3 with stepsize $h = 0.002$, the numerical errors of GPS and GPS2

Figure 5. For the Duffing oscillator computed by the GPS2 under a stepsize $h = 0.05$, (a) the response, and (b) showing the sign function

6.4 Duffing Oscillator

The Duffing equation under a forcing term is given by

$$\frac{d}{dt}\begin{bmatrix} x_1 \\ x_2 \end{bmatrix} = \begin{bmatrix} x_2 \\ -\gamma x_2 - \alpha x_1 - \beta x_1^3 + f_0 \cos \Omega t \end{bmatrix}, \tag{83}$$

where α, β and γ are physical parameters, and f_0 and ω are, respectively, the amplitude and circular frequency of external force. As shown in Figure 5(a) the numerical result is a chaos of the Duffing equation under the following parameters $\alpha = -1$, $\beta = 1$, $\gamma = 0.3$ and $\Omega = 1.2$, and $f_0 = 0.32$, where the time stepsize used is $h = 0.05$ and the time interval is $t \in [0, 800]$. The transient part of the trajectory is starting from the initial point $x_1 = 2$ and $x_2 = 0$. Under a larger $h = 0.05$ the GPS2 still preserves the chaotic structure very well; but, the GPS is not succeeded, and is blowing after $t = 800$ sec.

In Figure 5(b) we show the signum function defined by Equation (51) for this chaotic system, which switches irregularly and fast between $+1$ and -1.

6.5 Chua's Circuit

In order to assess the performance of the GPS2, we compute the following numerical example of Chua's circuit (Chua, 1982, 1986):

$$\begin{aligned} \dot{x} &= \alpha[y - h(x)], \\ \dot{y} &= x - y + z, \\ \dot{z} &= -\beta y, \end{aligned} \tag{84}$$

where h is a piecewise-linear function:

$$h(x) = \begin{cases} m_1 x + m_0 - m_1, & x \geq 1, \\ m_0 x, & |x| \leq 1, \\ m_1 x - m_0 + m_1, & x \leq -1. \end{cases} \tag{85}$$
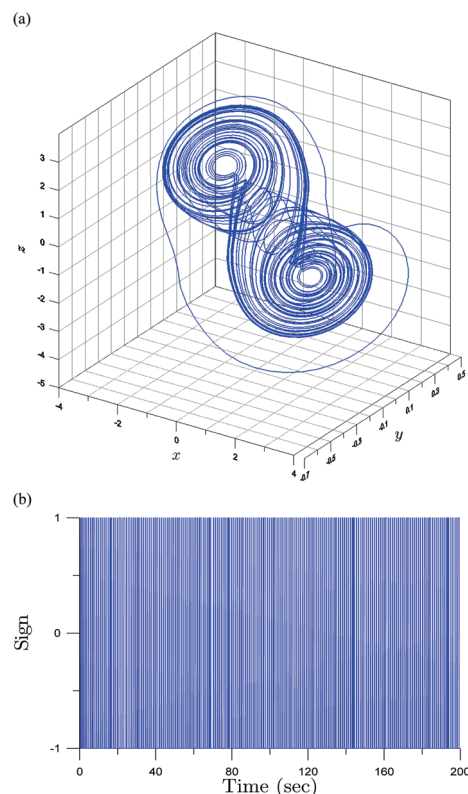

Figure 6. For Chua's circuit computed by the GPS2 under a stepsize $h = 0.01$, (a) the response, and (b) showing the sign function

The parameters are supposed to be $m_0 = -1/7$, $m_1 = 2/7$, $\alpha = 9$, and $\beta = 100/7$. The initial point is $(x(0), y(0), z(0)) = (2, 0, 0)$. In Figure 6(a) we show the scroll of (x, y, z) computed by the GPS2 with the step-size $h = 0.01$, where the time interval is $t \in [0, 200]$. It can be seen that the main feature of the scroll is revealed, which shows that the GPS2 can treat the chaotic problem with a larger time stepsize. In Figure 6(b) we show the signum function defined by Equation (51) for this chaotic system, which is fast switching between $+1$ and -1.

6.6 Lorenz Equations

In order to further assess the performance of the GPS2, we compute the following Lorenz equations (Lorenz, 1963):

$$
\begin{aligned}
\dot{x} &= \sigma(y - x), \\
\dot{y} &= \rho x - y - xz, \\
\dot{z} &= xy - \beta z,
\end{aligned}
\tag{86}
$$

where we fix $\sigma = 10$, $\rho = 28$ and $\beta = 8/3$ and the initial point is $(x(0), y(0), z(0)) = (1, 0, 1)$.
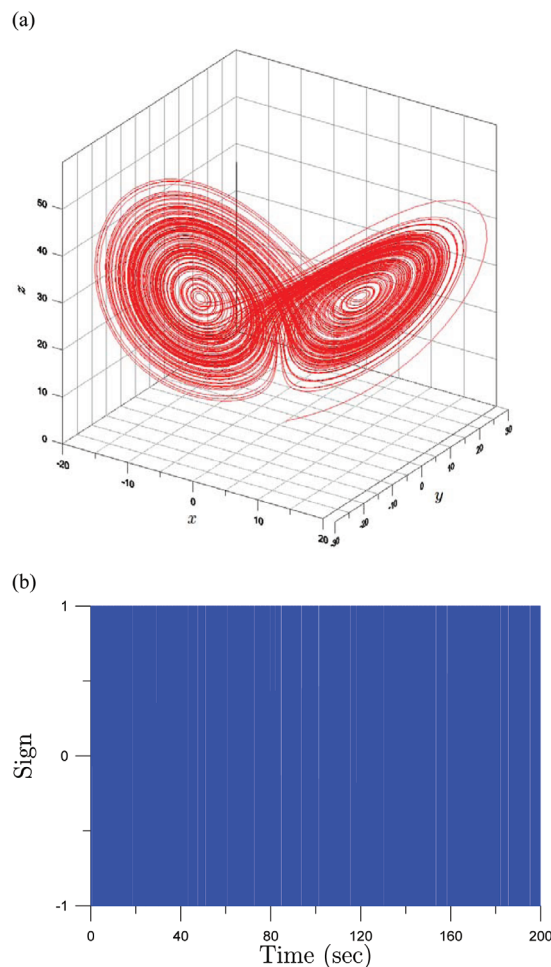
(a)

(b)

Figure 7. For Lorenz equations computed by the GPS2 under a stepsize $h = 0.01$, (a) the response, and (b) showing the sign function

In Figure 7(a) we show the butterfly of (x, y, z) computed by the GPS2 with the stepsize $h = 0.01$, where the time interval is $t \in [0, 200]$. In Figure 7(b) we show the signum function defined by Equation (51) for this chaotic system, which is irregularly and fast switching between $+1$ and -1.

6.7 Rössler Equations

Rössler (1976) has found a simple system, which is probably the most elementary geometric construction of chaos in continuous system by using stretch and fold:

$$
\begin{aligned}
\dot{x} &= -(y + z), \\
\dot{y} &= x + ay, \\
\dot{z} &= b + xz - cz,
\end{aligned}
\tag{87}
$$

where we fix $a = b = 1/5$ and $c = 5.7$, and the initial point is $(x(0), y(0), z(0)) = (-1, 0, 0)$.
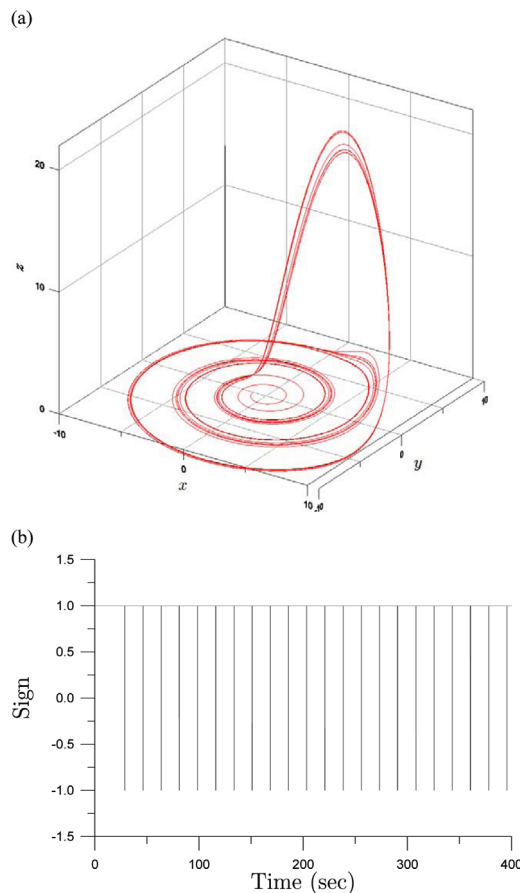
Figure 8. For Rössler equations computed by the GPS2 under a stepsize $h = 0.01$, (a) the response, and (b) showing the sign function

In Figure 8(a) we show the orbit of (x, y, z) computed by the GPS2 with the stepsize $h = 0.01$, where the time interval is $t \in [0, 400]$. In Figure 8(b) we show the signum function defined by Equation (51), which is in the state of $+1$ for most time, but sometimes it jumps to -1. When the orbit is in the folding state, the value of sign is $+1$, and when the orbit is in the stretching state sometimes (where z is fast raising to a large value) the value of sign is -1. From Figure 9 we can observe that the times of happening the stretch and the jumping from sign $= +1$ to sign $= -1$ are coincident. The signum function of the Rössler system is much simple and is quite different from those of other chaotic systems: the Duffing equations, Chua's equations and the Lorenz equations. The main reason for this phenomenon is that the Rössler system does not have the mechanism of *squeezing*, which together with the *folding* and the *stretching* constitute the three main mechanisms for *chaos*.

Remark 1 There are many effective methods like the power spectrum, the Lyapunov exponent, and the Poincaré map, to investigate the chaotic behavior of a given nonlinear dynamical system. Chen, Liu, and Chang (2007) have proposed a method by using the time sequence of η defined by Equation (15) to detect the chaos when they used the GPS to find the numerical solutions of Duffing equations, Lorenz equations and Rössler equations.

However, the criterion of η depends on the time stepsize h used in the numerical integration. The time sequence of sign($\|\mathbf{f}\|^2\|\mathbf{x}\|^2 - 2(\mathbf{f} \cdot \mathbf{x})^2$) used to detect the chaos is independent to the time stepsize, which is fully determined by the vector field and the orbit of the given nonlinear dynamical system.
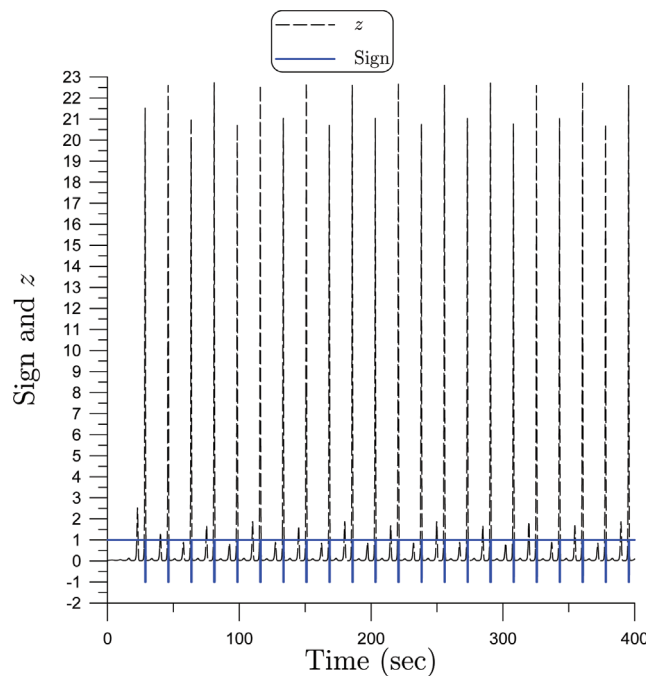

Figure 9. For Rössler equations comparing the value of z and the sign function in time

7. Conclusions

In this paper, the nonlinear ODEs system was converted into an augmented quasi-linear ODEs system in the Minkowski space, with the coefficient matrix being a Lie-form type. A full form of the Lie-algebra for the Lie-group $SO_o(n, 1)$ symmetry was provided. Based on this novel Lie-group symmetry of a full $SO_o(n, 1)$, we have deduced two closed-form solutions of the Lie-group $\mathbf{G} \in SO_o(n, 1)$, and the numerical algorithm to preserve the Lie-group properties at every time step was developed and proven. A signum function of sign($\|\mathbf{f}\|^2\|\mathbf{x}\|^2 - 2(\mathbf{f} \cdot \mathbf{x})^2$) was introduced. For the chaotic systems investigated in this paper the time sequence of sign was frequently switched between $+1$ and -1. Since the new method is easy to be implemented numerically and has good computational efficiency and accuracy, it can be used to find the numerical solution of nonlinear ODEs.

Acknowledgements

References

Chen, Y. W., Liu, C. S., & Chang, J. R. (2007). A chaos detectable and time step-size adaptive numerical scheme for non-linear dynamical systems. *J. Sound. Vib., 299*, 977-989. http://dx.doi.org/10.1016/j.jsv.2006.08.028

Chua, L. O., Hasler, M., Neirynck, J., & Verbugh, P. (1982). Dynamics of a piecewise-linear resonant circuit. *IEEE Trans. Circ. Sys., 29*, 535-547. http://dx.doi.org/10.1109/TCS.1982.1085192

Chua, L. O., Komuro, M., & Matsumoto, T. (1986). The double scroll family. *IEEE Trans. Circ. Sys., 33*, 1073-1118. http://dx.doi.org/10.1109/TCS.1986.1085869

Hairer, E., Lubich, C., & Wanner, C. (2002). *Geometric Numerical Integration: Structure-Preserving Algorithms for Ordinary Differential Equations*. Berlin: Springer-Verlag.

Hong, H. K., & Liu, C. S. (1999). Lorentz group $SO_o(5, 1)$ for perfect elastoplasticity with large deformation and a consistency numerical scheme. *Int. J. Non-Linear Mech., 34*, 1113-1130.

http://dx.doi.org/10.1016/S0020-7462(98)00081-X

Iserles, A. (1984). Solving linear ordinary differential equations by exponentials of iterated commutators. *Numer. Math., 45*, 183-199. http://dx.doi.org/10.1007/ BF01389464

Iserles, A., Munthe-Kaas, H. Z., Nørsett, S. P., & Zanna, A. (2000). Lie-group methods. *Acta Numerica, 9*, 215-365.

Iserles, A., & Nørsett, S. P. (1999). On the solution of linear differential equations in Lie groups. *Phil. Trans. Roy. Soc. Lond. A, 357*, 983-1019. http://dx.doi.org/10.1098/rsta.1999.0362

Iordanescu, R. (2007). Dynamical systems and Jordan structures. *Int. J. Pure Appl. Math., 35*, 125-143.

Iordanescu, R. (2009). *Jordan Structures in Analysis, Geometry and Physics*. Bucuresti: Editura Academiei Romane.

Lee, H. C., & Liu, C. S. (2009). The fourth-order group preserving methods for the integrations of ordinary differential equations. *Comput. Model. Eng. Sci., 41*, 1-26.

Liu, C. S. (2000). A Jordan algebra and dynamic system with associator as vector field. *Int. J. Non-Linear Mech., 35*, 421-429. http://dx.doi.org/10.1016/S0020-7462(99)00027-X

Liu, C. S. (2001). Cone of non-linear dynamical system and group preserving schemes. *Int. J. Non-Linear Mech., 36*, 1047-1068. http://dx.doi.org/10.1016/S0020-7462(00)00069-X

Liu, C. S. (2006). Preserving constraints of differential equations by numerical methods based on integrating factors. *Comput. Model. Eng. Sci., 12*, 83-107.

Liu, C. S. (2013a). A Lie-group $DSO(n)$ method for nonlinear dynamical systems. *Appl. Math. Lett., 26*, 710-717. http://dx.doi.org/10.1016/j.aml.2013.01.012

Liu, C. S. (2013b). A method of Lie-symmetry $GL(n, \mathbb{R})$ for solving non-linear dynamical systems. *Int. J. Non-Linear Mech., 52*, 85-95. http://dx.doi.org/10.1016/j.ijnonlinmec.2013.01.015

Lorenz, E. N. (1963). Deterministic nonperiodic flow. *J. Atmos. Sci., 20*, 130-141. http://dx.doi.org/10.1175/1520-0469(1963)020

Munthe-Kaas, H. Z. (1998). Runge-Kutta methods on Lie groups. *BIT, 38*, 92-111. http://dx.doi.org/10.1007/BF02510919

Munthe-Kaas, H. Z. (1999). High order Runge-Kutta methods on manifolds. *Appl. Numer. Math., 29*, 115-127. http://dx.doi.org/10.1016/S0168-9274(98)00030-0

Rössler, O. E. (1976). An equation for continuous chaos. *Phys. Lett. A, 35*, 397-398. http://dx.doi.org/10.1016/0375-9601(76)90101-8

Zhang, S., & Deng, Z. (2004). A simple and efficient fourth-order approximation solution for nonlinear dynamic system. *Mech. Res. Commu., 31*, 221-228. http://dx.doi.org/10.1016/j.mechrescom.2003.10.004

Zhang, S., & Deng, Z. (2006). Group preserving schemes for nonlinear dynamic system based on RKMK methods. *Appl. Math. Comput., 175*, 497-507. http://dx.doi.org/10.1016/j.amc.2005.07.062

Appendix A

In this Appendix we derive the solution of Equation (49). From the first-order ODEs (49) we have

$$
\begin{aligned}
\dot{z} &= a_0^2 w + c_0^2 y - c_0 z, \\
\dot{w} &= c_0 w + c_0 y - z, \\
\dot{y} &= c_0 w.
\end{aligned}
\tag{A1}
$$

It follows that

$$
\frac{d^3 y}{dt^3} + (a_0^2 - 2c_0^2)\dot{y} = 0.
\tag{A2}
$$

Depending on the value of $a_0^2 - 2c_0^2$, y has two different types of solutions.

For the first case with $a_0^2 - 2c_0^2 < 0$, i.e., sign $= -1$, we have

$$
y(t) = k_0 + k_1 f_1(t) + k_2 f_2(t),
\tag{A3}
$$

where k_0, k_1 and k_2 are constants and

$$
f_1(t) = \sinh(\omega t), \quad f_2(t) = \cosh(\omega t),
\tag{A4}
$$

in which $\omega = \sqrt{2c_0^2 - a_0^2}$.

Through some elementary operations we can derive the following solutions for z, w and y:

$$
\begin{pmatrix} z(t) \\ w(t) \\ y(t) \end{pmatrix} = \mathbf{P} \begin{pmatrix} z_0 \\ w_0 \\ y_0 \end{pmatrix},
$$

$$
\mathbf{P} = \begin{pmatrix}
c_2 + d_1 f_1 + c_3 f_2 & d_2 f_1 + d_3 f_2 - c_0 c_2 & c_2 \omega f_1 + c_1 c_2 (f_2 - 1) \\
-\frac{c_2 \omega f_1}{c_0^2} & \frac{c_2 \omega f_1}{c_0} + f_2 & \frac{c_2 \omega f_1}{c_0} \\
\frac{c_2(1 - f_2)}{c_0} & \frac{c_0 f_1}{\omega} + c_2(f_2 - 1) & c_3 + c_2 f_2(t)
\end{pmatrix},
\tag{A5}
$$

where z_0, w_0 and y_0 are initial values of z, w and y at an initial time $t = 0$, and

$$
\omega = \sqrt{2c_0^2 - a_0^2}, \quad c_1 = \frac{c_0^2 - \omega^2}{c_0}, \quad c_2 = \frac{c_0}{c_0 - c_1}, \quad c_3 = -\frac{c_1 c_2}{c_0},
$$

$$
d_1 = -\frac{c_2 \omega}{c_0}, \quad d_2 = \frac{c_0 c_1}{\omega} + c_2 \omega, \quad d_3 = c_0 + c_1 c_2.
\tag{A6}
$$

For the second case with $a_0^2 - 2c_0^2 > 0$, i.e., sign $= +1$, we have

$$
y(t) = k_0 + k_1 f_3(t) + k_2 f_4(t),
\tag{A7}
$$

where k_0, k_1 and k_2 are constants and

$$
f_3(t) = \sin(\omega t), \quad f_4(t) = \cos(\omega t),
\tag{A8}
$$

in which $\omega = \sqrt{a_0^2 - 2c_0^2}$.

Through some elementary operations we can derive the following solutions for z, w and y:

$$
\begin{pmatrix} z(t) \\ w(t) \\ y(t) \end{pmatrix} = \mathbf{Q} \begin{pmatrix} z_0 \\ w_0 \\ y_0 \end{pmatrix},
$$

$$
\mathbf{Q} = \begin{pmatrix}
c_2 + d_1 f_3 + c_3 f_4 & d_2 f_3 + d_3 f_4 - c_0 c_2 & c_1 c_2 (f_4 - 1) - c_2 \omega f_3 \\
\frac{c_2 \omega f_3}{c_0^2} & f_4 - \frac{c_2 \omega f_3}{c_0} & -\frac{c_2 \omega f_3}{c_0} \\
\frac{c_2(1 - f_4)}{c_0} & \frac{c_0 f_3}{\omega} + c_2(f_4 - 1) & c_3 + c_2 f_4
\end{pmatrix},
\tag{A9}
$$

where

$$\omega = \sqrt{a_0^2 - 2c_0^2}, \quad c_1 = \frac{c_0^2 + \omega^2}{c_0}, \quad c_2 = \frac{c_0}{c_0 - c_1}, \quad c_3 = -\frac{c_1 c_2}{c_0},$$
$$d_1 = \frac{c_2 \omega}{c_0}, \quad d_2 = \frac{c_0 c_1}{\omega} - c_2 \omega, \quad d_3 = c_0 + c_1 c_2. \tag{A10}$$

Copyrights